Hindawi Publishing Corporation
Journal of Nanomaterials
Volume 2012, Article ID 504026, 9 pages
doi:10.1155/2012/504026

Research Article

Synthesis of PEG-Iodine-Capped Gold Nanoparticles and Their Contrast Enhancement in *In Vitro* and *In Vivo* for X-Ray/CT

Sun-Hee Kim,[1,2,3] Eun-Mi Kim,[1,2,3] Chang-Moon Lee,[1,2,3] Dong Wook Kim,[1,2,3] Seok Tae Lim,[1,2,3] Myung-Hee Sohn,[1,2,3] and Hwan-Jeong Jeong[1,2,3]

[1] *Department of Nuclear Medicine, Chonbuk National University Hospital, Dukjin-gu, Jeonju, Geumam-dong 634-18, Republic of Korea*
[2] *Cyclotron Research Center, Chonbuk National University Hospital, Dukjin-gu, Jeonju, Geumam-dong 634-18, Republic of Korea*
[3] *Research Institute of Clinical Medicine, Chonbuk National University Medical School and Hospital, Dukjin-gu, Jeonju, Geumam-dong 634-18, Republic of Korea*

Correspondence should be addressed to Hwan-Jeong Jeong, jayjeong@chonbuk.ac.kr

Received 23 November 2011; Accepted 31 January 2012

Academic Editor: Zhifei Dai

We designed gold nanoparticles (AuNPs) capped with iodine and polyethylene glycol (PEG) to provide effective enhancement for X-ray CT imaging. The methoxy PEG-iodine-capped AuNPs were prepared through the chemisorption of iodine and substitution of methoxy PEG-SH onto the surface of gold nanoparticles, and severe aggregation in TEM was not observed. The binding energies of Au $4f_{7/2}$ and I $3d_{5/2}$ of the methoxy PEG-iodine-capped AuNPs were obtained as 84.1 eV and 619.3 eV, respectively. The binding energy shift of methoxy PEG-iodine-capped AuNPs would be resulted from the chemisorption between gold nanoparticles and iodine atoms. The methoxy PEG-iodine-capped AuNPs have higher enhancement compared to PEG-capped gold nanoparicles in the same amount of gold *in vitro*. After postinjection of methoxy PEG-iodine-capped AuNPs into the mice, dramatic contrast enhancement at the heart, aorta, liver, and kidney was observed, this was maintained up to 5 days, and there was no evidence of apparent toxicity. In conclusion, methoxy PEG-iodine-capped AuNPs might be a good candidate as a CT contrast agent for blood pool imaging, and this will also contribute to the prolongation of a blood circulation time for X-ray CT imaging.

1. Introduction

X-ray computed tomography (CT) has been widely used as an imaging tool for noninvasive diagnosis of many diseases. Water-soluble iodinated ionic and nonionic small molecules are commonly used as CT contrast agents more than 10 years [1–6]. However, CT contrast agents containing iodine have got disadvantages, in which contrast agents are excreted from the body very rapidly, nonspecific, and have renal toxicity. Various contrast agents based on nanoparticles have recently been developed to overcome the short circulation time of iodinated contrast agents. Gold nanoparticles are an example of such CT contrast agent. It is well known that gold has a higher atomic number ($_{79}$Au versus $_{53}$I) and a greater absorption coefficient than iodine (k edge; Au, 80.7 keV versus I, 33 keV) [7, 8]. During the past few years, biocompatible polymer-capped nanoparticles or water-soluble macromolecular nanoparticles have been investigated for suitability as CT contrast agents in nanomaterials and nanomedicine [9–13]. Gold nanoparticles have been used for the detection of target materials by exploiting the optical properties of aggregation of gold with the desired substrates [14–20]. These nanoparticles with different targeting ligands can be used as drugs and for gene delivery into cells in various diagnostic and therapeutic research settings [21–27]. Gold and iodine atoms have an additional interesting feature: halide ions and organic compounds absorb onto the transition-metal surfaces through mutual interactions [28–32]. This absorption can result in more stable complexes.

The preparation of gold nanoparticles through the citrate reduction method generally increased the stability of colloidal gold nanoparticles via the absorption of citrate ions onto the surfaces of the gold nanoparticles [33, 34]. The absorbed materials are linked to the surfaces and form

a layer of absorbed molecules. For example, self-assembled monolayer (SAM) products of gold nanoparticles are often formed via chemisorptions of the thiol (–SH) functional group by the gold surface [35–39]. Halide ions and various organic or inorganic compounds can be absorbed by the metal surfaces. Chemisorption is one class of absorption that is driven by a chemical reaction that creates strong new bonds at the exposed metal surfaces. Because the nature of chemisorptions differs from system to system, the chemisorptions of a metal depend on its chemical identity and surface structure.

Gold halide is well known to have a peculiar electron system, and halide ions are known to have different affinities to gold surfaces [40]. The relative binding strengths of gold halides are I > Br > Cl [41, 42]. The addition of iodide ions to gold nanoparticles leads to aggregation and fusion of gold nanoparticles [43–45]. This suggests that gold nanoparticles with iodide are capable of not only being displaced but are also stabilized by the organic or inorganic materials.

In this study, we report the preparation of gold nanoparticles with iodine using chemisorptions of iodine onto the surface of gold, resulting in a CT contrast agent that can be used for *in vivo* blood-pool imaging.

2. Experimental

2.1. Chemicals. Hydrogen tetrachloroaurate(III) trihydrate ($HAuCl_4 \cdot 3H_2O$), sodium citrate tribasic dihydrate, and sodium iodide (NaI) were purchased from Sigma-Aldrich chemicals (St. Louis, MO, USA). All chemicals were used without further purification. Methoxy polyethylene glycol sulfhydryl 5000 was purchased from SunBio (Anyang, South Korea). Milli-Q water (18.2 MΩ) was used in all the preparation. $Na^{125}I$ was obtained from Perkin Elmer Life Science, Inc. (Boston, MA, USA). Optiray320 was obtained from our hospital (320 mg of iodine per milliliter, Tyco healthcare, Montreal, Canada).

2.2. Preparation of the Colloidal Gold Nanoparticles. The colloidal gold nanoparticles were prepared using the following method [10]. Gold chloride trihydrate (0.050 g; 1.27×10^{-4} mole) was dissolved in 500 mL deionized water. Sodium citrate tribasic dihydrate solution (17.5 mL of a 1% solution) was added to the refluxed gold chloride solution as a reducing agent, followed by reflux and vigorous stirring for another 15 min. Sodium citrate solution caused an instant color change of the mixture to wine-red. The prepared colloidal gold nanoparticles had a 10 nm core diameter.

2.3. Preparation of the Methoxy PEG-Capped AuNPs. A 0.105 g (2.10×10^{-5} mole) of methoxy PEG sulfhydryl 5000 solution was dissolved in 20 mL deionized water and added to the prepared colloidal gold nanoparticles, followed by gentle stirring for 12 h at room temperature. The reaction solution was collected using a centrifugal filter (molecular weight cut off: 50 kDa, Millipore Corporation, Billerica, MA, USA) and washed three times with deionized water.

2.4. Preparation of the PEG-Iodine-Capped AuNPs. Sodium iodide solution (0.01 M; 25 mL) was combined with the prepared citrate ion-capped gold nanoparticles and was gently stirred at room temperature for 1 h. Methoxy PEG sulfhydryl 5000 solution was then added to the iodine-capped gold nanoparticles solution and stirred gently for 12 h at room temperature. The final solution was concentrated using a centrifugal filter and washed three times with deionized water. The condensed iodine-containing products were stabilized with methoxy PEG sulfhydryl.

2.5. Characterization of the Methoxy PEG-Capped AuNPs and the Methoxy PEG-Iodine-Capped AuNPs. The absorption spectra of the methoxy PEG-capped AuNPs and the methoxy PEG-iodine-capped AuNPs were assessed using a UV-visible spectrophotometer (HP 8453, Hewlett Packed, Germany). The surface compositional atoms of the gold nanoparticles were characterized using X-ray photoelectron spectroscopy (XPS) (AXIS-NOVA, Kratos, MC, UK). The X-ray source was monochromatic A1Kσ, 1486.6 eV. The sizes and shapes of the methoxy PEG-capped AuNPs and the methoxy PEG-iodine-capped AuNPs were observed with transmission electron microscope (TEM) (H-7650; Hitachi, Tokyo, Japan). The samples were prepared commercially onto copper grids bearing formvar carbon film (FCF200-Cu: Electron Microscopy Science, Hatfield, PA, USA). The hydrodynamic particles sizes of the methoxy PEG-capped AuNPs and the methoxy PEG-iodine-capped AuNPs in water were measured using dynamic light scattering (DLS) (Microtrac-UP150; Microtrac, Largo, FL, USA). The concentrations of gold in the AuNPs were measured using an inductively coupled plasma mass spectrometer (ICP-MS) (Agilent 7500a; Agilent Technologies, Santa Clara, CA, USA).

2.6. Static Image of Methoxy PEG-^{125}Iodine-Capped Gold Nanoparticles. The colloidal gold nanoparticles were prepared using citrate reduction method and a preparation of methoxy PEG-^{125}Iodine-capped (660 μCi, 38 ng) gold nanoparticles were then progressed using a radioactive isotope to confirm an existence of iodine on the surface of gold nanoparticles. Iodine-125 gamma camera imaging and imaging processing were performed using a small-animal imaging system with pinhole collimation (aperture diameter = 1 mm; focal length = 9 cm) and a 15- to 45-keV photopeak energy window (X-SPECT/CT, GE Healthcare, Uppsala, Sweden).

2.7. In Vitro Experiments. An in vitro experiment was performed to compare the degree of contrast enhancements of the methoxy PEG-capped AuNPs and the methoxy PEG-iodine-capped AuNPs at the same concentration of gold and to determine the relative CT attenuation of the methoxy PEG-iodine AuNPs compared with that of the commercial iodinated contrast agent (Optiray^{TM}320, Tyco Healthcare, Canada). Optiray320 was prepared with serially diluted samples in distilled water. The serial samples contained the following amounts of iodine per milliliter: (a) 5.04×10^{-4} mole; (b) 2.52×10^{-4} mole; (c) 1.26×10^{-4} mole; (d)

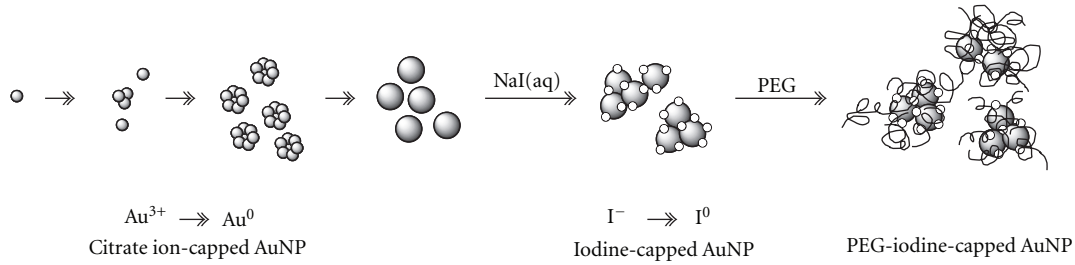

Figure 1: Synthetic scheme of methoxy PEG-iodine-capped AuNPs. First, the initial Au^0 atoms generated using the citrate reduction method were assembled to form stabilized citrate ion-capped AuNPs. Second, the colloidal gold nanoparticles were reacted with iodide ions in sodium iodide solution. Finally, methoxy PEG-SH was added to the iodine-capped AuNPs solution, and AuNPs was stabilized by methoxy PEG-SH.

6.30×10^{-5} mole; (e) water (control). The concentration of gold was determined by ICP-MS to be 3.70×10^{-5} mole. All samples were placed in 200 μL PCR tubes. The CT images were acquired using a CT scanner (X-SPECT/CT, GE Healthcare, Uppsala, Sweden) with an estimated X-ray power of 75 kVp. The final reconstructed images were converted to digital images with the AMIRA software 3.1 (San Diego, CA, USA).

2.8. Acquisition of CT Imaging in Mice. All animal experiments were performed in compliance with the policies and procedures of the Institutional Animal Care and Use Committee for animal treatment of Chonbuk National University. A female balb/c mouse (6 wks, weighting 25 g) was purchased from Orient Bio Inc., (Seongnam, South Korea) and was used in the animal study. The degree of contrast enhancement of the methoxy PEG-iodine-capped AuNPs was assessed *in vivo*. The mouse was anesthetized in an induction chamber with 2% isoflurane in oxygen and was maintained in 1.5% isoflurane in oxygen during CT imaging. The methoxy PEG-iodine-capped AuNPs were injected into the mouse via a catheter in the tail vein. The images were acquired at 30 m, 60 m, 1, 2, 6, 12, 24, 48, and 120 h after postinjection. The CT images were acquired using X-SPECT/CT with an estimated X-ray power of 75 kVp. The final reconstructed images were converted to digital images with the AMIRA software 3.1.

3. Results and Discussion

The design of the procedure for the preparation of methoxy polyethylene glycol (PEG)-iodine-capped gold nanoparticles (AuNPs) is shown in Figure 1. The methoxy PEG-capped AuNPs and the methoxy PEG-iodine-capped AuNPs were prepared according to Figure 1 and were observed to be deep red-wine-colored solutions. Figure 2 showed characteristic surface plasmon resonance (SPR) bands of methoxy PEG-capped AuNPs and methoxy PEG-iodine-capped AuNPs at the different wavelengths 520 and 521 nm. The SPR bands of the gold nanoparticles showed red shifts from 518 nm to 520 and 521 nm due to chemisorption between the sulfhydryl (–SH) group and the iodine on the surfaces of the gold nanoparticles. The chemisorption of PEG-SH on the surfaces of gold nanoparticles contributed to the stabilization of these

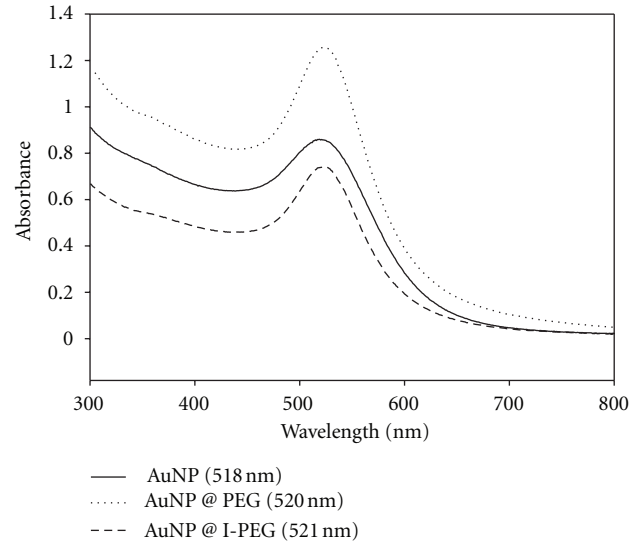

Figure 2: UV-visible absorption spectra of the citrate ion-capped AuNPs (solid line), methoxy PEG-capped AuNPs (dotted line) and the methoxy PEG-iodine-capped AuNPs (medium-dashed line).

gold nanoparticles. The substitution of PEG-SH onto gold nanoparticles resulted in the release of citrate ions from the surfaces of the gold nanoparticles. The chemisorption of iodine also induced changes in the surface charges of the gold nanoparticles, resulting in the assembly of gold nanoparticles. As a result, the red shifts of the SPR bands of gold nanoparticles were observed in UV-visible absorption spectra.

The sizes and shapes of the prepared gold nanoparticles were confirmed using transmission electron microscopy (TEM) and dynamic light scattering (DLS) as shown in Figures 3 and 4. The methoxy PEG-capped AuNPs had an average core diameter of 10 nm and were dispersed uniformly, but the methoxy PEG-iodine-capped AuNPs were slightly aggregated due to the addition of iodide ion during the preparation procedure (Figure 3(d)). The adsorbent iodide ions in aqueous sodium iodide induced the aggregation of gold nanoparticles [43]. The hydrodynamic size distributions of the methoxy PEG-capped AuNPs and the methoxy PEG-iodine-capped AuNPs in water were measured using DLS. The sizes of the AuNPs were confirmed as

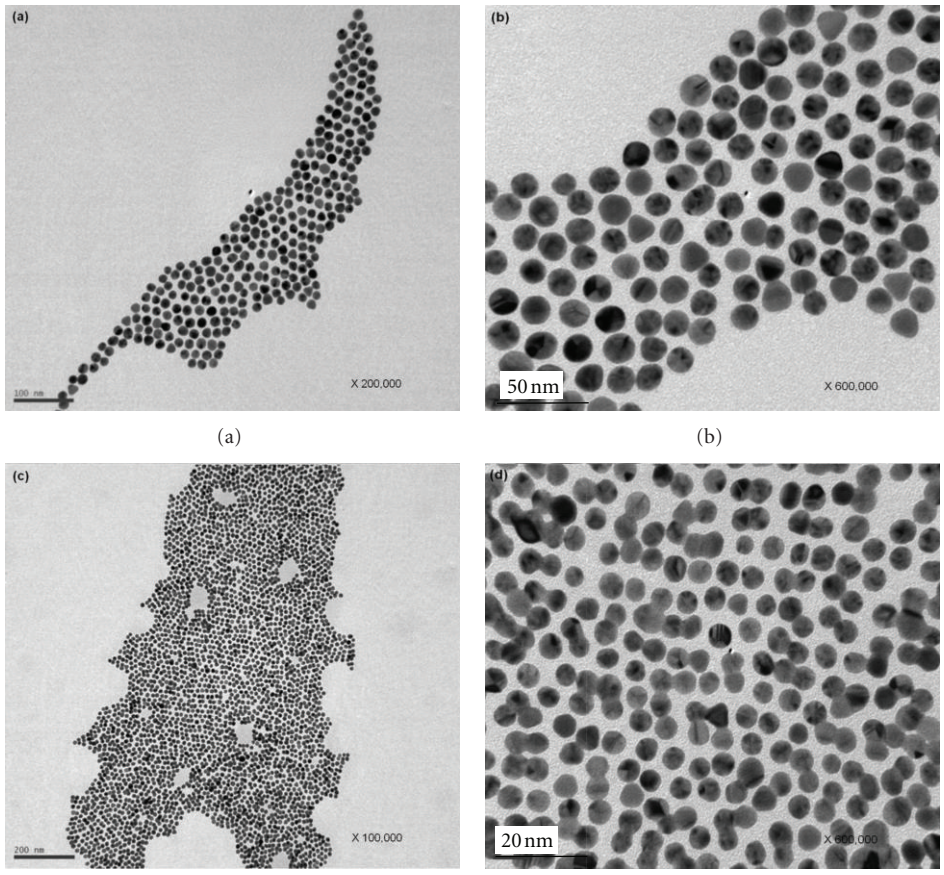

(a) (b) (c) (d)

Figure 3: TEM images of methoxy PEG-capped AuNPs with scale bar 100 nm (a), methoxy PEG-capped AuNPs with scale bar 50 nm (b), methoxy PEG-iodine-capped AuNPs with scale bar 200 nm (c), and methoxy PEG-iodine-capped AuNPs with scale bar 20 nm (d).

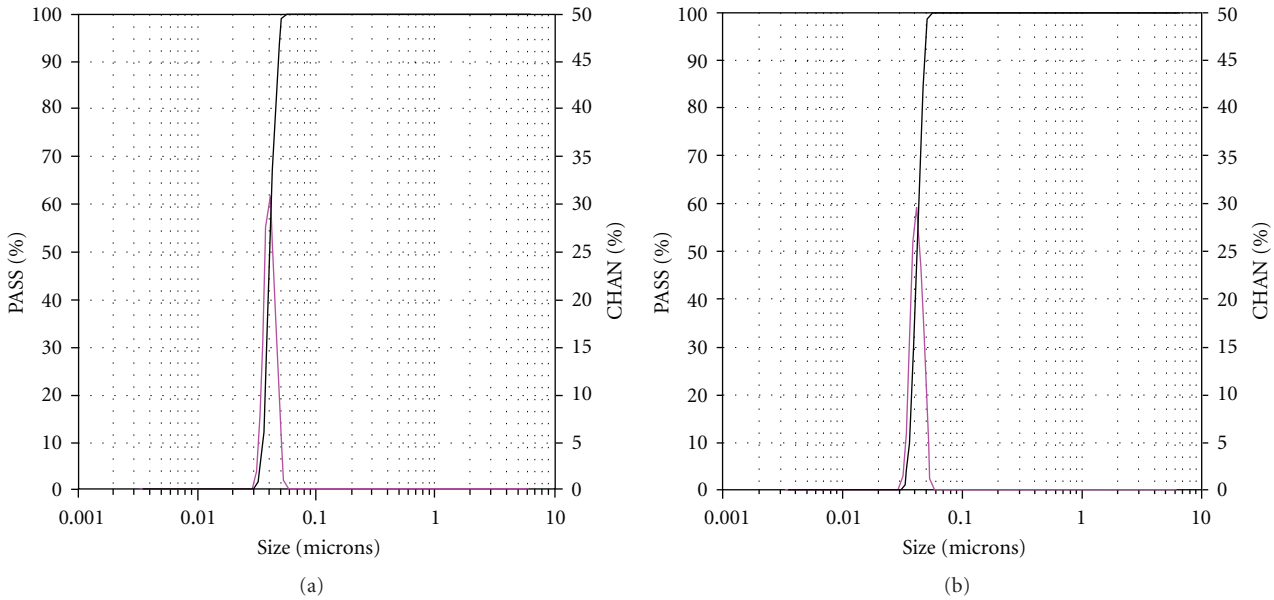

Figure 4: Dynamic light scattering (DLS) spectra of methoxy PEG-capped AuNPs (a) and methoxy PEG-iodine-capped AuNPs (b). The average mean diameter of (a) was 40 nm, and that of (b) was 41 nm.

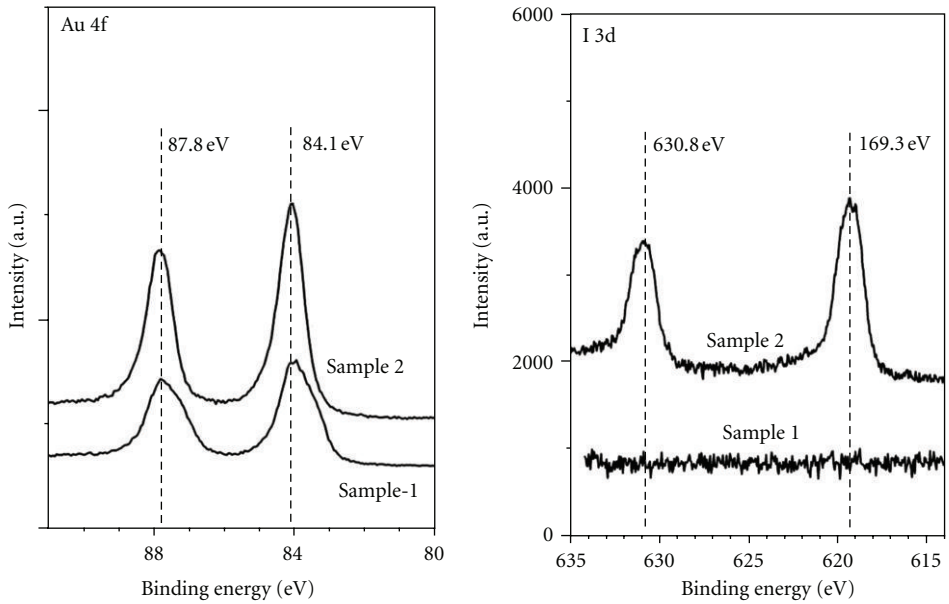

Figure 5: X-ray photoelectron spectroscopic (XPS) data for the methoxy PEG-capped AuNPs (sample-1) and the methoxy PEG-iodine-capped AuNPs (sample-2). These data show the change of binding energy of gold and iodine.

Table 1: X-ray photoelectron spectroscopic data analysis for gold (Au) and iodine (I). XPS analysis shows the existence of iodine on the surfaces of gold nanoparticles.

Component	Binding energy (eV)	
	Au	I
	$4f_{7/2}$	$3d_{5/2}$
Au	83.8[a]	—
Au-I	83.9 ± 0.5[b]	618.3 ± 0.5[c]
AuNP@PEG	84.0	—
AuNP@I-PEG	84.1	619.3

[a,b,c]The binding energies for Au and Au-I are from [29].

40 nm and 41 nm, respectively (Figure 4). The surface stress of gold nanoparticles was increased due to the mismatch between iodine and gold, leading to the slight aggregation of gold nanoparticles [44]. Because iodine was added to gold nanoparticles within a short time period (one hour), sodium iodide prevented the severe aggregation of gold nanoparticles, and then the methoxy PEG-iodine-capped AuNPs were stabilized via capping with methoxy PEG-SH.

The components of the methoxy PEG-iodine-capped AuNPs and the methoxy PEG-capped AuNPs were investigated using X-ray photoelectron spectroscopy (XPS). The metal-halide coordinated complex is thought to involve a strong bond. Iodide ions underwent spontaneous oxidation to generate neutral iodine atoms, zero-valent iodine, in aqueous sodium iodide [28, 43]. The newly formed iodine could be absorbed onto the surfaces of gold nanoparticles by virtue of their strong affinity. Iodine replaced citrate ions on the gold nanoparticles through chemisorption. Binding energy values for gold and iodine were investigated in Figure 5. The Au $4f_{7/2}$ and $4f_{5/2}$ spectra of the methoxy PEG-iodine-capped AuNPs (sample 2) were obtained at 84.1 eV and 87.8 eV, respectively. The binding energy of Au $4f_{7/2}$ was changed slightly from 83.8 eV to 84.1 eV through treatment with iodine. According to a previous report, the characteristic binding energy of Au $4f_{7/2}$, gold (Au) is 83.8 eV if untreated with iodine and that of Au $4f_{7/2}$ in a gold-iodine interface is 83.9 ± 0.5 eV (Table 1) [29]. After the chemisorption of iodine to gold nanoparticles, the binding energy of gold in nanoparticles increased slightly as expected from the change in the level of gold-iodine complex described in the literature. The binding energy of Au $4f_{7/2}$ in the methoxy PEG-capped AuNPs (sample 1) also changed from 83.8 eV to 84.0 eV. This shifted binding energy was ascribed to the AuNP-PEG assemblies representing the bonded thiol (–SH) of PEG-SH with gold nanoparticles. These results indicate that the changes of binding energy of the methoxy PEG-capped AuNPs and methoxy PEG-iodine-capped AuNPs was resulted by chemisorption via thiol (–SH) and iodine. Iodine, $3d_{5/2}$ and $3d_{3/2}$ spectra were clearly visible in the methoxy PEG-iodine-capped AuNPs due to the formation of gold-iodine bonds at 619.3 eV and 630.8 eV. However, the energy of iodine $3d_{5/2}$ was not clearly observed in the methoxy PEG-capped AuNPs. The binding energy of iodine in gold-iodide is known to be 618.3 ± 0.5 [28]. After the addition reaction of iodine, the band of iodine $3d_{5/2}$ was shifted higher, from 618.3 eV to 619.3 eV. In this study, the iodine species that were generated were established as iodine (I_2) molecules. These results indicate that there was no gold-iodide (Au-I) complex with inserted iodide ions (I^-). Judging from the these results, we suggest that the binding of neutral iodine (I_2) molecules to gold nanoparticles is more favorable than the combination of iodide ions (I^-)

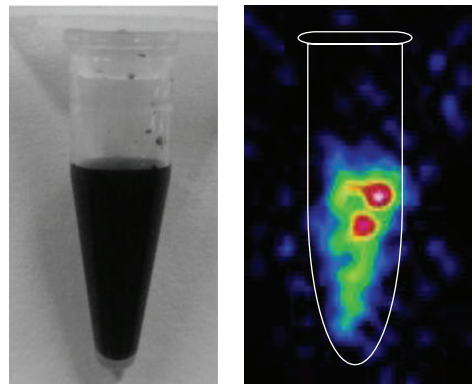

(a) (b)

Figure 6: The methoxy PEG-^{125}iodine-capped gold nanoparticles showed high radioactive through the static image. Photographic image of methoxy PEG-^{12}iodine-capped gold nanoparticles (a) and static image of methoxy PEG-^{125}iodine-capped gold nanoparticles (b).

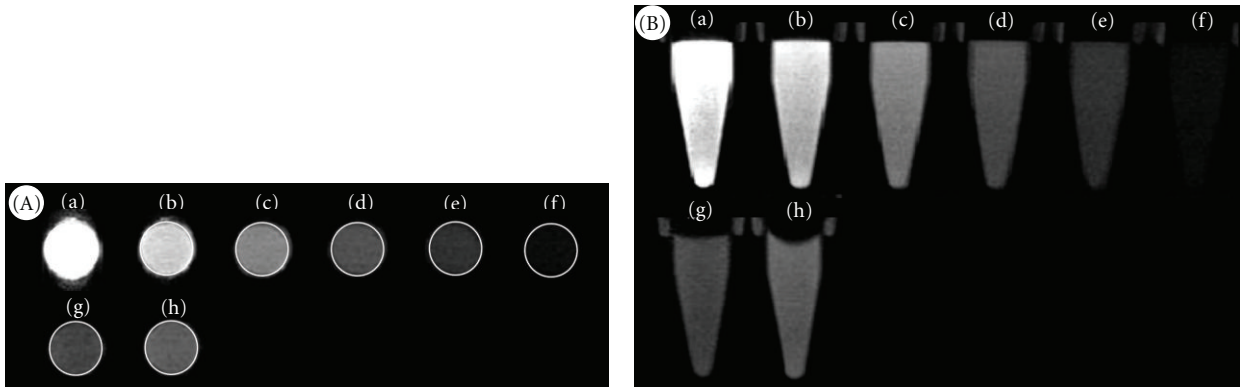

Figure 7: X-ray CT *in vitro* images. Optiray320 was prepared with serially diluted samples in distilled water. The serial samples contained the following amounts of iodine per milliliter: (a) 5.04×10^{-4} mole (943 HU); (b) 2.52×10^{-4} mole (400 HU); (c) 1.26×10^{-4} mole (100 HU); (d) 6.30×10^{-5} mole (41 HU); (e) water; (f) empty tube. The gold concentrations of (g) methoxy PEG-capped AuNPs (177 HU) and (h) methoxy PEG-iodine-capped AuNPs (301 HU) were determined by ICP-MS to be 3.70×10^{-5} mole. Axial images (A) and coronal images (B), respectively.

and gold nanoparticles (Au^0), and that the iodine-capped gold nanoparticles were stabilized through addition of the methoxy PEG-SH. It was also derived an evidence of ^{125}I on the surface of gold nanoparticles from the analysis of the static images. This result indicates that the gold nanoparticles were combined with radioactive iodine as shown in Figure 6. The contrast enhancements of methoxy PEG-capped AuNPs and methoxy PEG-iodine-capped AuNPs were compared *in vitro* for the same amount of gold (3.70×10^{-5} mole, Au) as shown in Figure 7. The result was high-contrast enhancement in methoxy PEG-iodine-capped AuNPs compared to that of methoxy PEG-capped AuNPs. At the same concentration of gold, a higher-contrast enhancement of methoxy PEG-iodine-capped AuNPs than methoxy PEG-capped AuNPs was considered to be due to iodine on the surfaces of the gold nanoparticles. In Figure 7, the iodine contents of the (c) and (d) samples were 1.25×10^{-4} mole and 6.30×10^{-5} moles, respectively. As shown in Figures 7(d) and 7(g), 3.70×10^{-5} mole gold amount in methoxy PEG-capped AuNPs has shown almost similar enhancement with 6.30×10^{-5} mole iodine concentration. On the other hand, contrast of methoxy PEG-iodine-capped AuNPs was shown higher than (c) and lower than (d) concentration. Therefore, with the analysis of acquired images of tube samples, we could derive the amount of iodide, although we did not check its iodide exactly, in methoxy PEG-iodine-capped AuNPs to above 6.30×10^{-5} mole. When comparing by atom concentration additionally, methoxy PEG-iodine-capped AuNPs was 1.7 times lower than Optiray320, but contrast intensity has shown almost the same signal.

We observed obvious contrast enhancement at the heart, aorta, liver, and kidney after injection compared with that of the untreated control as shown in Figure 8. The contrast enhancement was shown for 24 h in the aorta. We found that methoxy PEG-iodine-capped AuNPs cleared from the heart after 48 h after injection and were taken up by the reticuloendothelial system (RES) system in the liver. The renal artery and renal pelvis were also observed vividly. The degree of contrast enhancement of methoxy PEG-iodine-capped AuNPs was maintained from immediately up

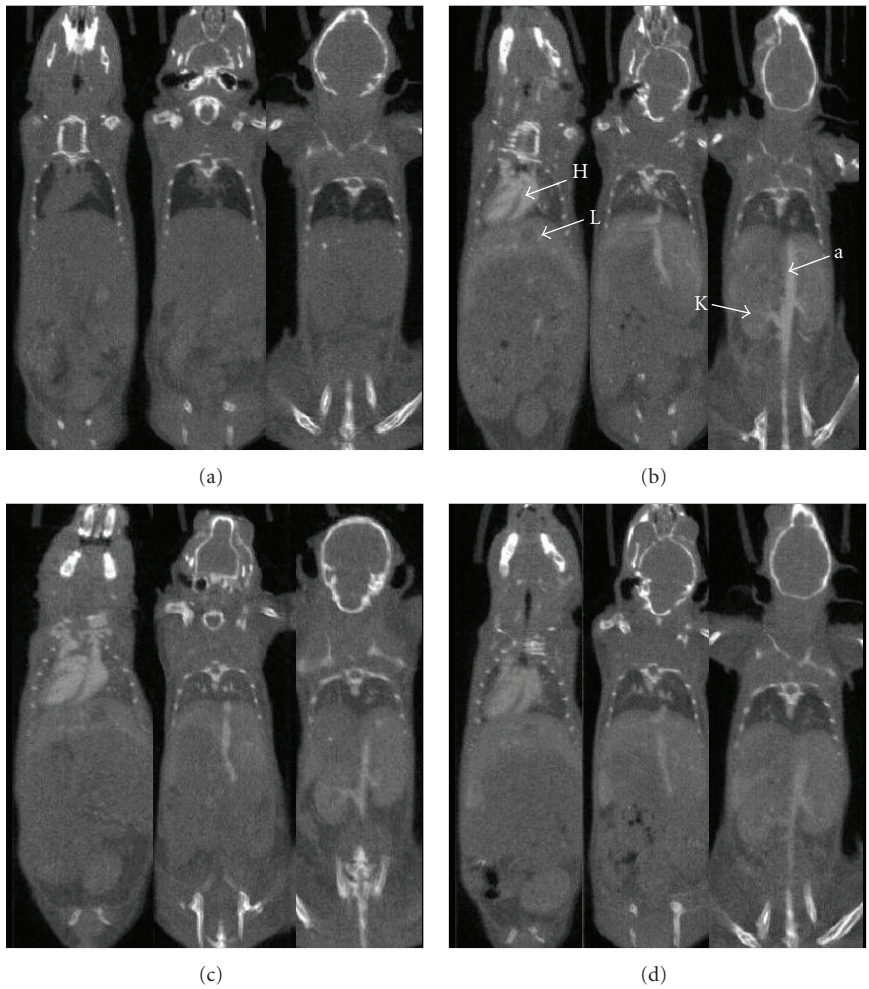

Figure 8: X-ray images in mice. (a) before injection, (b) immediately, (c) 30 m, and (d) 24 h after post-tail vein injection of methoxy PEG-iodine-capped AuNPs (Au amount: 56 μmole). The heart, aorta, kidney, and liver were enhanced, respectively. The arrows indicate H: heart, L: liver, K: kidney, and a: aorta, respectively.

to 5 days after injection at the same position. From the above results, we confirmed that the methoxy PEG-iodine-capped AuNPs prolonged a significant blood circulation time compared with the commercialized contrast agent with iodine. The CT images were displayed in sequence according to the time-dependence in Figure 8. There was no evidence of apparent toxicity for the duration of the enhancement.

4. Conclusions

In this study, we described the preparation of new concept of PEG-iodine capped gold nanoparticles using the chemisorption mechanism of iodine atoms onto the surface of gold nanoparticles, and this was stabilized with methoxy PEG-SH. The additional method of iodine capping on the gold nanoparticles brought about better enhancement for X-ray compared to iodine non-capped gold nanoparticle, and the quality of X-ray/CT imaging of polymer-capped gold-iodine complex was more improved compared to Optiray320 in spite of using smaller doses. One of the problems for using the conventional contrast agents in X-ray imaging is that large amounts of the current polyiodinated contrast agents are required to obtain the appropriate enhancement and the other short blood circulation time of them. New concept of iodine capping onto gold nanoparticles would be a good candidate for solving these problems.

Authors' Contribution

S.-H. Kim and E.-M. Kim contributed equally to this paper.

Acknowledgments

This paper was supported by a Grant from the National R&D program for Cancer Control, Ministry for Health, Welfare and Family Affairs, Republic of Korea (no. 0626220) and National Research Foundation of Korea (NRF) grant funded by the Korea government (MEST) (No. 2011-0028581).

References

[1] S. B. Yu and A. D. Watson, "Metal-based X-ray contrast media," *Chemical Reviews*, vol. 99, no. 9, pp. 2353–2377, 1999.

[2] T. Wharton and L. J. Wilson, "Highly-iodinated fullerene as a contrast agent for X-ray imaging," *Bioorganic and Medicinal Chemistry*, vol. 10, no. 11, pp. 3545–3554, 2002.

[3] F. Mottu, D. A. Rüfenacht, A. Laurent, and E. Doelker, "Iodine-containing cellulose mixed esters as radiopaque polymers for direct embolization of cerebral aneurysms and arteriovenous malformations," *Biomaterials*, vol. 23, no. 1, pp. 121–131, 2002.

[4] C. Zaharia, T. Zecheru, M. F. Moreau et al., "Chemical structure of methylmethacrylate-2-[2′,3′,5′-triiodobenzoyl]oxoethyl methacrylate copolymer, radio-opacity, in vitro and in vivo biocompatibility," *Acta Biomaterialia*, vol. 4, no. 6, pp. 1762–1769, 2008.

[5] A. Galperin, D. Margel, J. Baniel, G. Dank, H. Biton, and S. Margel, "Radiopaque iodinated polymeric nanoparticles for X-ray imaging applications," *Biomaterials*, vol. 28, no. 30, pp. 4461–4468, 2007.

[6] U. Rode and R. Müller, "Transformation of the ionic X-ray contrast agent diatrizoate and related triiodinated benzoates by Trametes versicolor," *Applied and Environmental Microbiology*, vol. 64, no. 8, pp. 3114–3117, 1998.

[7] J. F. Hainfeld, D. N. Slatkin, T. M. Focella, and H. M. Smilowitz, "Gold nanoparticles: a new X-ray contrast agent," *British Journal of Radiology*, vol. 79, no. 939, pp. 248–253, 2006.

[8] M. C. Daniel and D. Astruc, "Gold nanoparticles: assembly, supramolecular chemistry, quantum-size-related properties, and applications toward biology, catalysis, and nanotechnology," *Chemical Reviews*, vol. 104, no. 1, pp. 293–346, 2004.

[9] D. Kim, S. Park, H. L. Jae, Y. J. Yong, and S. Jon, "Antibiofouling polymer-coated gold nanoparticles as a contrast agent for in vivo X-ray computed tomography imaging," *Journal of the American Chemical Society*, vol. 129, no. 24, pp. 7661–7665, 2007.

[10] Q. Y. Cai, S. H. Kim, K. S. Choi et al., "Colloidal gold nanoparticles as a blood-pool contrast agent for x-ray computed tomography in mice," *Investigative Radiology*, vol. 42, no. 12, pp. 797–806, 2007.

[11] H. Wang, L. Zheng, C. Peng et al., "Computed tomography imaging of cancer cells using acetylated dendrimer-entrapped gold nanoparticles," *Biomaterials*, vol. 32, no. 11, pp. 2979–2988, 2011.

[12] C. Peng, L. Zheng, Q. Chen et al., "PEGylated dendrimer-entrapped gold nanoparticles for in vivo blood pool and tumor imaging by computed tomography," *Biomaterials*, vol. 33, no. 4, pp. 1107–1119, 2012.

[13] C. Kojima, Y. Umeda, M. Ogawa, A. Harada, Y. Magata, and K. Kono, "X-ray computed tomography contrast agents prepared by seeded growth of gold nanoparticles in PEGylated dendrimer," *Nanotechnology*, vol. 21, no. 24, Article ID 245104, 2010.

[14] R. Elghanian, J. J. Storhoff, R. C. Mucic, R. L. Letsinger, and C. A. Mirkin, "Selective colorimetric detection of polynucleotides based on the distance-dependent optical properties of gold nanoparticles," *Science*, vol. 277, no. 5329, pp. 1078–1081, 1997.

[15] X. Xu, M. S. Han, and C. A. Mirkin, "A gold-nanoparticle-based real-time colorimetric screening method for endonuclease activity and inhibition," *Angewandte Chemie - International Edition*, vol. 46, no. 19, pp. 3468–3470, 2007.

[16] C. D. Medley, J. E. Smith, Z. Tang, Y. Wu, S. Bamrungsap, and W. Tan, "Gold nanoparticle-based colorimetric assay for the direct detection of cancerous cells," *Analytical Chemistry*, vol. 80, no. 4, pp. 1067–1072, 2008.

[17] J. Wang, Y. Cao, Y. Xu, and G. Li, "Colorimetric multiplexed immunoassay for sequential detection of tumor markers," *Biosensors and Bioelectronics*, vol. 25, no. 2, pp. 532–536, 2009.

[18] H. Lee, T. Kang, K. A. Yoon, S. Y. Lee, S. W. Joo, and K. Lee, "Colorimetric detection of mutations in epidermal growth factor receptor using gold nanoparticle aggregation," *Biosensors & bioelectronics*, vol. 25, no. 7, pp. 1669–1674, 2010.

[19] J. H. Kang, Y. Asami, M. Murata et al., "Gold nanoparticle-based colorimetric assay for cancer diagnosis," *Biosensors and Bioelectronics*, vol. 25, no. 8, pp. 1869–1874, 2010.

[20] H. Li and L. Rothberg, "Colorimetric detection of DNA sequences based on electrostatic interactions with unmodified gold nanoparticles," *Proceedings of the National Academy of Sciences of the United States of America*, vol. 101, no. 39, pp. 14036–14039, 2004.

[21] P. Baptista, E. Pereira, P. Eaton et al., "Gold nanoparticles for the development of clinical diagnosis methods," *Analytical and Bioanalytical Chemistry*, vol. 391, no. 3, pp. 943–950, 2008.

[22] R. Popovtzer, A. Agrawal, N. A. Kotov et al., "Targeted gold nanoparticles enable molecular CT imaging of cancer," *Nano Letters*, vol. 8, no. 12, pp. 4593–4596, 2008.

[23] S. Dhar, W. L. Daniel, D. A. Giljohann, C. A. Mirkin, and S. J. Lippard, "Polyvalent oligonucleotide gold nanoparticle conjugates as delivery vehicles for platinum(IV) warheads," *Journal of the American Chemical Society*, vol. 131, no. 41, pp. 14652–14653, 2009.

[24] R. Guo, L. Zhang, H. Qian, R. Li, X. Jiang, and B. Liu, "Multifunctional nanocarriers for cell imaging, drug delivery, and near-IR photothermal therapy," *Langmuir*, vol. 26, no. 8, pp. 5428–5434, 2010.

[25] Z. Zhang, J. Jia, Y. Lai, Y. Ma, J. Weng, and L. Sun, "Conjugating folic acid to gold nanoparticles through glutathione for targeting and detecting cancer cells," *Bioorganic and Medicinal Chemistry*, vol. 18, no. 15, pp. 5528–5534, 2010.

[26] E. C. Dreaden, S. C. Mwakwari, Q. H. Sodji, A. K. Oyelere, and M. A. El-Sayed, "Tamoxifen-poly(ethylene glycol)-thiol gold nanoparticle conjugates: enhanced potency and selective delivery for breast cancer treatment," *Bioconjugate Chemistry*, vol. 20, no. 12, pp. 2247–2253, 2009.

[27] D. Pan, T. A. Williams, A. Senpan et al., "Detecting vascular biosignatures with a colloidal, radio-opaque polymeric nanoparticle," *Journal of the American Chemical Society*, vol. 131, no. 42, pp. 15522–15527, 2009.

[28] P. Pyykkö, "Theoretical chemistry of gold. II," *Inorganica Chimica Acta*, vol. 358, no. 14, pp. 4113–4130, 2005.

[29] G. M. Berry, M. E. Bothwell, B. G. Bravo et al., "Spectroscopic and electrochemical studies of iodine coordinated to noble-metal electrode surfaces," *Langmuir*, vol. 5, no. 3, pp. 707–713, 1989.

[30] P. A. M. Teirlinck and F. W. Petersen, "The nature of gold-iodide adsorption onto coconut-shell carbon," *Minerals Engineering*, vol. 9, no. 9, pp. 923–930, 1996.

[31] D. K. Smith, N. R. Miller, and B. A. Korgel, "Iodide in CTAB prevents gold nanorod formation," *Langmuir*, vol. 25, no. 16, pp. 9518–9524, 2009.

[32] A. Zhang, X. Tie, J. Zhang, Y. An, and L. Li, "Adsorption of iodide and iodate on colloidal silver surface," *Applied Surface Science*, vol. 255, no. 5, pp. 3184–3187, 2008.

[33] S. K. Balasubramanian, L. Yang, L. Y. L. Yung, C. N. Ong, W. Y. Ong, and L. E. Yu, "Characterization, purification, and

stability of gold nanoparticles," *Biomaterials*, vol. 31, no. 34, pp. 9023–9030, 2010.

[34] J. Kunze, I. Burgess, R. Nichols, C. Buess-Herman, and J. Lipkowski, "Electrochemical evaluation of citrate adsorption on Au(111) and the stability of citrate-reduced gold colloids," *Journal of Electroanalytical Chemistry*, vol. 599, no. 2, pp. 147–159, 2007.

[35] J. R. Reimers, Y. Wang, B. O. Cankurtaran, and M. J. Ford, "Chemical analysis of the superatom model for sulfur-stabilized gold nanoparticles," *Journal of the American Chemical Society*, vol. 132, no. 24, pp. 8378–8384, 2010.

[36] C. J. Zhong and M. D. Porter, "Fine structure in the voltammetric desorption curves of alkanethiolate monolayers chemisorbed at gold," *Journal of Electroanalytical Chemistry*, vol. 425, no. 1-2, pp. 147–153, 1997.

[37] W. R. Thompson, M. Cai, M. Ho, and J. E. Pemberton, "Hydrolysis and condensation of self-assembled monolayers of (3-mercaptopropyl)trimethoxysilane on Ag and Au surfaces," *Langmuir*, vol. 13, no. 8, pp. 2291–2302, 1997.

[38] H. McCormick, R. McMillan, K. Merrett et al., "XPS study of the effect of the conditions of peptide chemisorption to gold and silver coated polymer surfaces," *Colloids and Surfaces B*, vol. 26, no. 4, pp. 351–363, 2002.

[39] D. R. Blasini, R. J. Tremont, N. Batina, I. González, and C. R. Cabrera, "Self-assembly of (3-mercaptopropyl)trimethoxysilane on iodine coated gold electrodes," *Journal of Electroanalytical Chemistry*, vol. 540, pp. 45–52, 2003.

[40] T. Kamata, T. Kawasaki, T. Kodzasa et al., "Third order nonlinear optical properties of gold iodide with a long alkyl chain," *Synthetic Metals*, vol. 102, no. 1–3, pp. 1560–1561, 1999.

[41] O. M. Magnussen, B. M. Ocko, J. X. Wang, and R. R. Adzic, "In-situ X-ray diffraction and STM studies of bromide sdsorption on Au(111) electrodes," *Journal of Physical Chemistry*, vol. 100, no. 13, pp. 5500–5508, 1996.

[42] Y. Liu, L. Liu, and R. Guo, "Br–induced facile fabrication of spongelike gold/amino acid nanocomposites and their applications in surface-enhanced raman scattering," *Langmuir*, vol. 26, no. 16, pp. 13479–13485, 2010.

[43] W. Cheng, S. Dong, and E. Wang, "Iodine-induced gold-nanoparticle fusion/fragmentation/aggregation and iodine-linked nanostructured assemblies on a glass substrate," *Angewandte Chemie - International Edition*, vol. 42, no. 4, pp. 449–452, 2003.

[44] J. Wang, Y. F. Li, and C. Z. Huang, "Identification of iodine-induced morphological transformation of gold nanorods," *Journal of Physical Chemistry C*, vol. 112, no. 31, pp. 11691–11695, 2008.

[45] S. Singh, R. Pasricha, U. M. Bhatta, P. V. Satyam, M. Sastry, and B. L. V. Prasad, "Effect of halogen addition to monolayer protected gold nanoparticles," *Journal of Materials Chemistry*, vol. 17, no. 16, pp. 1614–1619, 2007.